

## Softened Hydrophobic Attraction between Macroscopic Surfaces in Relative Motion

Xueyan Zhang, Yingxi Zhu, and Steve Granick\*

Department of Materials Science and Engineering  
University of Illinois at Urbana-Champaign  
1304 West Green Street, Urbana, Illinois 61801

Received April 6, 2001

Revised Manuscript Received May 18, 2001

A puzzling aspect of the hydrophobic attraction is that its intensity and range appear to be qualitatively different as concerns extended surfaces of large area and small molecules of modest size.<sup>1–4</sup> One difference is fundamental: the hydrogen-bond network of water is believed for theoretical reasons to be less disrupted near a single alkane molecule than near an extended surface.<sup>1–4</sup> A second difference is phenomenological: direct measurement shows attractive forces between extended surfaces starting at separations too large to be reasonably explained by disruption of the hydrogen-bond network. This conclusion comes from 20 years of research using the surface forces apparatus (SFA) and, more recently, atomic force microscopy (AFM). The onset of attraction,  $\sim 10$  nm in the first experiments,<sup>5–8</sup> soon increased by nearly an order of magnitude<sup>9–11</sup> and has been reported, in the most recent work, to begin at separations as large as 500 nm.<sup>12</sup> This has engendered much speculation because it is unreasonably large, compared to the size of the water molecule ( $\sim 0.25$  nm). The range of interaction lessens if the system (water and the hydrophobic surfaces) is carefully degassed.<sup>13–17</sup> Water in usual laboratory experiments is not degassed, however, and therefore, it is relevant to understand the origin of long-range attraction in that environment. A recent review summarizes the experimental and theoretical situation.<sup>11</sup>

In the course of experiments intended to probe the predicted slip of water over hydrophobic surfaces,<sup>18,19</sup> we have observed that the long-range hydrophobic force was weakened to the point of vanishing when the solid surfaces experienced low-level vibrations around a mean static separation. This Communication quantifies the effect and its dependence on velocity. We conclude by discussing the possible implications.

Details of the modified surface forces apparatus were described elsewhere.<sup>20</sup> Briefly, the spacing between atomically smooth sheets of mica was measured with a resolution of 0.2–0.5 nm using optical interferometry, and using piezoelectric actuators, nanometer-level oscillatory modulations of film spacing were also made. The amplitude and frequency of modulation were controlled independently, allowing the mean velocity to vary over a wide range without large change of the film thickness. The temperature was 25 °C. The water was filtered and deionized by passage through filtration columns (Nanopure).

Two methods were used to produce hydrophobic surfaces. Initially, freshly cleaved muscovite mica was coated by self-assembly with a methyl-terminated monolayer of condensed octadecyltriethoxysiloxane (OTE).<sup>21</sup> However, the incidence of surface gel particles (which prevented approach to strict monolayer–monolayer contact) was reduced when OTE was spread at the air–water interface, hydrolyzed, and transferred onto mica using Langmuir–Blodgett methods adapted from the work of Takahara et al.<sup>22</sup> This was accomplished by spreading OTE onto  $3.2 \times 10^{-3}$  M HCl (pH = 2.5), waiting 0.5 h for hydrolysis, slowly compressing to the surface pressure  $\pi = 20$  mN·m<sup>-1</sup> (3–4 h), and transferring the close-packed film onto mica by the Langmuir–Blodgett technique at a creep-up speed of 2 mm·min<sup>-1</sup>. Finally the transferred films were vacuum-baked at 120 °C for 2 h. Results presented below involve surfaces prepared using the latter preparation. The interferometric thickness of the resulting close-packed monolayer was 2.5 nm. The contact angle was  $\sim 110^\circ$  with  $< 2^\circ$  hysteresis.

The manner in which hydrophobic surfaces are prepared is plainly of great importance and can generate a wide range of experimental results.<sup>5–17</sup> It was our experience that the range of attraction increased as the monolayers were made to be increasingly free of defects. The range of forces described below is about twice as large as in our own initial findings using OTE monolayers that had a larger defect density. The dependence on defect density was not explored explicitly. Instead, the main point of the experiments presented below is to show the strong dependence on harmonic velocity when the same pairs of surfaces were studied such that differences between methods of surface preparation were normalized out.

The attraction recorded during the approach of OTE surfaces with a droplet of deionized water between is plotted in Figure 1 as a function of surface–surface separation ( $D$ ). Force is normalized by the mean radius of curvature  $R$  of the mica cylinders ( $R \approx 2$  cm). Here,  $D = 0$  refers to monolayer–monolayer contact in air. In water, the surfaces jumped into adhesive contact at  $3 \pm 2$  Å. The slope of the force–distance curves equals the spring constant of the force-measuring spring, indicating by well-known arguments<sup>5–10</sup> that they represented a spring instability (see caption to Figure 1). This “jump-in” was very slow to develop, however. It was found necessary to equilibrate each point for  $\sim 3$ –10 min at the largest levels of thickness. At lesser thickness the equilibration accelerated, and finally a jump into contact was observed. The pull-off force to separate the surfaces from contact at rest (113 mN·m<sup>-1</sup> in Figure 1) implies, from the JKR theory,<sup>12</sup> the surface energy of about 12 mJ·m<sup>-2</sup> (and up to about 30% less than this when oscillations were applied). The onset of attraction at 650 nm for the hydrophobic surfaces at rest is somewhat larger than in any past study of which we are aware. However, we emphasize that the

(1) Huang, D. M.; Chandler, D. *Proc. Natl. Acad. Sci. U.S.A.* **2000**, *97*, 8324.

(2) Lum, K.; Chandler, D.; Weeks, J. D. *J. Phys. Chem. B.* **1999**, *103*, 4570.

(3) Stillinger, F. H. *J. Solution Chem.* **1973**, *2*, 141.

(4) Lee, C. Y.; McCammon, J. A. *J. Chem. Phys.* **1984**, *80*, 4448.

(5) Israelachvili, J. N.; Pashley, R. M. *Nature* **1982**, *300*, 341; *J. Colloid Interface Sci.* **1984**, *98*, 500.

(6) Pashley, R. M.; McGuiggan, P. M.; Ninham, B. W.; Evans, D. F. *Science* **1985**, *229*, 1088.

(7) Claesson, P. M.; Blom, C. E.; Herder, P. C.; Ninham, B. W. *J. Colloid Interface Sci.* **1986**, *114*, 234.

(8) Tsao, Y.-H.; Evans, D. F.; Wennerström, H. *Science* **1993**, *262*, 547.

(9) Claesson, P. M.; Christenson, H. K. *J. Phys. Chem.* **1988**, *92*, 1650.

(10) Christenson, H. K.; Claesson, P. M.; Berg, J.; Herder, P. C. *J. Phys. Chem.* **1989**, *93*, 1472.

(11) Spalla, O. *Curr. Opin. Colloid Interface Sci.* **2000**, *5*, 5 and references therein.

(12) Considine, R. F.; Drummond, C. J. *Langmuir* **2000**, *16*, 631.

(13) Ishida, N.; Sakamoto, M.; Miyahara, M.; Higashitani, K. *Langmuir* **2000**, *16*, 5681.

(14) Wood, J.; Sharma, R. *Langmuir* **1995**, *11*, 4797.

(15) Parker, J. L.; Claesson, P. M.; Attard, P. *J. Phys. Chem.* **1994**, *98*, 8468; Carambassis, A.; Jonker, L. C.; Attard, P.; Rutland, M. W. *Phys. Rev. Lett.* **1998**, *80*, 5357; Attard, P. *Langmuir* **2000**, *16*, 4455.

(16) Craig, V. S. J.; Ninham, B. W.; Pashley, R. M. *Langmuir* **1999**, *15*, 1562.

(17) Considine, R. F.; Hayes, R. A.; Horn, R. G. *Langmuir* **1999**, *15*, 1657.

(18) Vinogradova, O. I. *Langmuir* **1995**, *11*, 2213.

(19) Zhu, Y.; Granick S. *MRS Symp.* **2001**, *651*, in press.

(20) Dhinojwala, A.; Granick, S. *Macromolecules* **1997**, *30*, 1079.

(21) Peanasky, J. S.; Schneider, H. M.; Granick, S.; Kessel, C. R. *Langmuir* **1995**, *11*, 953.

(22) Takahara, A.; Kojio, K.; Ge, S.; Kajiyama, T. *J. Vac. Sci. Technol.* **1996**, *A14* (3), 1747.

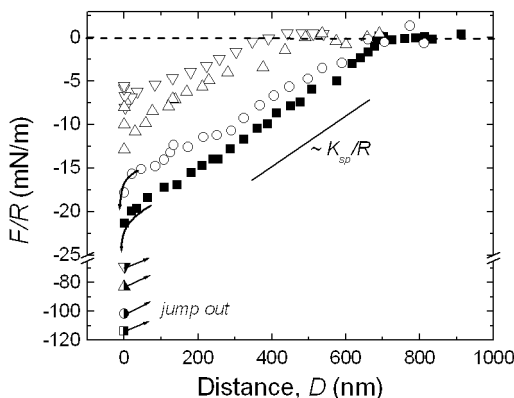


**Figure 1.** Force–distance profiles of deionized water between hydrophobic surfaces (OTE monolayers on mica). Force  $F$ , normalized by the mean radius of curvature ( $R \approx 2$  cm) of the crossed cylinders, is plotted against surface separation. Forces were measured during approach from static deflection of the force-measuring spring, while simultaneously applying small-amplitude harmonic oscillations in the normal direction with peak velocity  $v_{\text{peak}} = d \times 2\pi f$ , where  $d$  denotes displacement amplitude and  $f$  denotes frequency. This was zero (solid squares),  $7.6 \text{ nm}\cdot\text{s}^{-1}$  ( $d = 1.6 \text{ nm}$ ,  $f = 0.76 \text{ Hz}$ ; circles),  $26 \text{ nm}\cdot\text{s}^{-1}$  ( $d = 3.2 \text{ nm}$ ,  $f = 1.3 \text{ Hz}$ ; up triangles),  $52 \text{ nm}\cdot\text{s}^{-1}$  ( $d = 3.2 \text{ nm}$ ,  $f = 2.6 \text{ Hz}$ ; down triangles). The pull-off adhesion forces (“jump out”), measured at rest and with oscillation, are indicated by respective semi-filled symbols. The approach data follow the straight line with slope  $K_{\text{sp}}/R$  (drawn separately as a guide to the eye), indicating that they represented a spring instability (“jump in”) such that the gradient of attractive force exceeded the spring constant ( $K_{\text{sp}}$ ),  $930 \text{ N}\cdot\text{m}^{-1}$ .

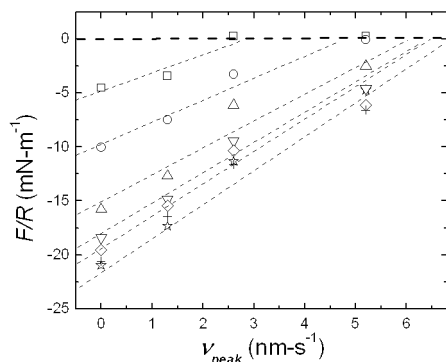


**Figure 2.** Attractive force ( $F/R$ ) at seven different surface separations ( $D$ ) is plotted against peak velocity. The film thickness was  $D = 720 \text{ nm}$  (squares),  $540 \text{ nm}$  (circles),  $228 \text{ nm}$  (upper triangles),  $116 \text{ nm}$  (down triangles),  $63 \text{ nm}$  (diamonds),  $17 \text{ nm}$  (crosses),  $5 \text{ nm}$  (stars).

level of pull-off force was consistent with the prior findings of other groups using other systems.<sup>5–17</sup>

In Figure 2, the force  $F$  at a given surface separation  $D$  is plotted against peak velocity ( $v_{\text{peak}}$ ) during nanometer-level vibration of the film spacing at several values of  $D$ . It diminished with increasing velocity, and its magnitude at a given  $D$  appeared in every instance to extrapolate smoothly to zero. The possible role of hydrodynamic forces was considered but discarded as a possible explanation. By using the Reynolds equation to estimate the hydrodynamic force due to the applied oscillatory vibrations in the normal direction,<sup>19,20</sup> the hydrodynamic forces were found to be insignificant over this range of harmonic velocity, amounting to not more than 1–2% of the measured static force.

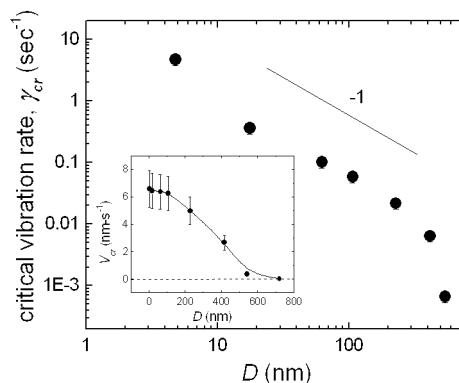


**Figure 3.** Extrapolated critical vibration rate ( $v_{\text{cr}}/D$ ), at which  $F/R$  plotted in Figure 2 extrapolates to zero, is plotted against surface separation  $D$  on log–log scales. Error bars are shown, and the slope of  $-1$  is drawn as a guide to the eye. Inset shows the extrapolated critical velocity ( $v_{\text{cr}}$ ) plotted against  $D$  on linear scales.

These observations clearly imply some kind of rate-dependent process. To estimate its time scale, the critical velocity ( $v_c$ ) was calculated, at which  $F \rightarrow 0$ . It was normalized by the length scale of this problem, which is the film thickness,  $D$ . This quantity, the critical vibration rate, should be roughly the inverse of a characteristic time (possibly a bubble formation time; see below). In Figure 3 it is plotted against film thickness on log–log scales. One sees that at short-range it increased as  $D^{-1}$  ( $D < 10 \text{ nm}$ ) and at long-range more strongly. Note that the velocity-weakening effect was observed at distances as small as 5–10 nm. These comprise distances where hydrophobic attraction has been reported between extended surfaces at rest even when water and surfaces were reported to be degassed.<sup>13,14</sup> In future work, parallel experiments using degassed water will be important. This was not feasible in this study to date because water could not be maintained degassed with confidence during the equilibration of several hours in our force-measuring device.

Similar results (not shown) were also obtained when the surfaces were vibrated parallel to one another rather than in the normal direction. Some precedence is found in a recent AFM study that reported weakened hydrophobic adhesion force with increasing approach rate.<sup>17</sup>

These observations remove some of the discrepancy between the range of hydrophobic forces between extended surfaces of macroscopic size<sup>5–17</sup> and the range that is expected theoretically.<sup>1–4</sup> A tentative explanation is based on the frequent suggestion that the long-range hydrophobic attraction between extended surfaces stems from the action of microscopic or submicron-sized bubbles that arise either from spontaneous cavitation or the presence of adventitious air droplets that form bridges between the opposed surfaces.<sup>11,13,15–17</sup> The experiments reported here show that this effect required time to develop. Hydrophobic attraction at long-range was softened to the point of vanishing when the solid surfaces were not stationary.

**Acknowledgment.** This material is based upon work supported by the National Science Foundation (Tribology Program) and by U.S. Department of Energy, Division of Materials Sciences under Award No. DEFG9645439, through the Frederick Seitz Materials Research Laboratory at the University of Illinois at Urbana-Champaign.

JA015960F